Rheol Acta 36:406–415 (1997)

ORIGINAL CONTRIBUTION

Nino Grizzuti
Ottavio Bifulco

Effects of coalescence and breakup on the steady-state morphology of an immiscible polymer blend in shear flow

Received: 2 December 1996
Accepted: 10 April 1997

Dr. N. Grizzuti (✉) · O. Bifulco
Dipartimento di Ingegneria Chimica
Università degli Studi di Napoli "Federico II"
Piazzale V. Tecchio, 80
80125 Napoli, Italy
E-mail: grizzuti@ds.unina.it

Abstract The steady-state morphology of an immiscible polymer blend in shear flow has been investigated by optical microscopy techniques. The blend is composed by poly-isobutylene (PIB) and poly-dimethylsiloxane (PDMS) of comparable viscosity. Experiments were performed by means of a home-made transparent parallel plate device. The two plates can be independently counter-rotated, so that sheared droplets of the dispersed phase can be kept fixed with respect to the microscope point of view, and observed for long times. The distribution of drops and their average size were measured directly during flow at different shear rates and for different blend compositions. It was found that the average drop size in steady-state conditions is a decreasing function of the applied shear rate, and does not depend on blend composition for volume fractions up to 10%. Experiments have proved that, in the shear rate range which could be investigated, the stationary morphology is controlled only by coalescence phenomena, droplet breakup playing no role in determining the size of the dispersed phase. More generally, it has been shown that the steady-state morphology is a function not only of the physical parameters of the blend and of the shear rate, but also of the initial conditions applied to the blend. The steady-state results reported in this paper constitute the first direct experimental confirmation of theoretical models which describe the mechanisms of shear-induced drop coalescence.

Key words Polymer blends – shear flow – morphology – coalescence – breakup

Introduction

Blending of polymers is an efficient way to produce materials with specific properties (Utracki, 1989). Blending can be useful to obtain plastics with improved physical properties, such as rubber filled polymers (Wu, 1987), or to increase melt processability, for example, when small amounts of a liquid crystalline polymer are added to a thermoplastic material to reduce its viscosity (Cogswell et al., 1983; Collyer, 1996). In all cases, the blend material properties are strongly affected by its local morphology. In fact, most polymers are thermodynamically incompatible (Krause, 1978), and the blending process gives rise to a heterogeneous microstructure which can be characterized by the size, shape and distribution of the constitutive domains. Typically, the blend morphology is formed by inclusions of one polymer (the dispersed phase) embedded in a matrix formed by the other polymer (the continuous phase). In static conditions, the dispersed inclusions generally assume a spherical drop shape, due to the action of the interfacial tension.

The final morphology of a blend is determined by the flow conditions applied in the liquid state (Elmendorp, 1991). In a sufficiently concentrated system, two main flow-induced phenomena control the size of the morphology: one drop can deform and eventually breakup into smaller entities; conversely, two or more droplets can collide and eventually coalesce to form

RA 836

one larger domain. The importance of flow conditions on blend morphology would make a direct observation of these phenomena highly desirable. This is not possible for most commercial blends, because of lack of transparency of the components. Further experimental limits are connected to the intrinsic turbidity of the blends (due to light scattering generated by the dispersed drops), and to the high processing temperatures. For these reasons, a huge number of literature studies has inferred the effect of flow on the morphology by examining the blend microstructure in the solid state, where different techniques (optical and electron microscopy, selective etching, etc.) are available. A classical example of such a research route can be found in the recent work by Sundararaj and Macosko (1995). Typically, this "post-mortem" type of morphology evaluation is aimed at characterizing blends when processed in industrial conditions. For this reason, the majority of the literature data have been obtained for not well controlled flow conditions, such as those encountered in batch mixers (Favis and Chalifoux, 1987), capillary or slit dies (Rivera-Gastélum and Wagner, 1996), extruders (Utracki and Shi, 1992). In most cases, therefore, only qualitative relations between morphology size and flow parameters (e.g., shear rate) have been proposed.

Due to the above-mentioned experimental difficulties, in situ morphology measurements of polymer blends in well controlled flow conditions are relatively scarce in the literature. Starting from the pioneering work of Taylor (1934), optical microscopy techniques have been applied to study the deformation and breakup of droplets both in shear and elongational flow (see, for example, Chaffey et al., 1965; Karam and Bellinger, 1968; Gauthier et al., 1971; Chin and Han, 1980). All these studies, however, have been focused on the case of isolated drops. As a consequence, only deformation and breakup phenomena were considered, since coalescence, by definition, can only take place in concentrated blends. Multi-drop systems have been investigated by light scattering methods (Lingaae-Jorgensen and Utracki, 1991). Such a technique, however, is limited to low concentrations of the dispersed phase (about 1%), due to multiple scattering. Even in this case, therefore, coalescence is expected to play a minor role. More recently, Takahashi and Noda (1995) performed optical microscopy measurements of the average drop size in a model polymer blend undergoing steady shear flow. Although limited to the single case of a 50% blend composition, their results provided the first direct evidence of the role that both coalescence and breakup phenomena play in determining the flowing blend morphology.

In the attempt to directly relate the microstructure of relatively concentrated blends to the flow conditions, in this paper we performed real-time, in situ observations of the morphology of an immiscible polymer blend undergoing steady shear flow. Experiments have been carried out on a model blend constituted of poly-isobutylene and poly-dimethylsiloxane, both liquids at room temperature. The drop size distribution generated under controlled steady-state shear flow has been quantitatively measured. Experimental results have been compared with existing theories for both coalescence and breakup, in order to clarify the effects of the two mechanisms on the size of the blend morphology in steady-state conditions. It must be mentioned here that the same model blend has been used by Vinckier et al. (1996) to probe the flow-induced morphology by means of rheological measurements.

Experimental

Incompatible blends were prepared from poly-isobutylene (PIB, Parapol 1300 from Exxon) and poly-dimethylsiloxane (PDMS, Rhodorsil 47V200000 from Rhône-Poulenc). These model polymers were selected because they are transparent liquids at room temperature. Additionally, a relatively large difference in their refractive index ($\Delta n \approx 0.09$, see Table 1) guarantees an easy, direct observation of the interface and of its evolution during flow by optical microscopy techniques. At the same time, their viscosity is sufficiently high so as to make their blend behavior similar to that of commercial thermoplastic systems.

Blends of PIB and PDMS were prepared by two different techniques. In one case, the two components were fed to a miniature, Kenics-type static mixer (Cole-Parmer) by means of two independent syringe pumps (Harvard Apparatus, mod. 909). By suitably setting the pump flow rate, blends of the desired composition could be obtained. In the other case, blends were prepared by hand-mixing small weighted amounts of the two polymers in a beaker with a spatula. Blends produced by the first technique were completely free of air bubbles, whereas those produced by hand-mixing incorporated much air, which was removed by an overnight stay under vacuum. The manual procedure generated a better dispersed blend, with drops mostly in the micron and sub-micron size range, whereas the static mixer was able to produce a droplet mean size in the range 3–10 μm. Blends prepared with both methods were used, and no influence of the mixing procedure on the final results was observed. Four PIB/PDMS blends were prepared, indicated by 2.5/97.5, 5/95, 10/90, 90/10, the first number representing the percent volume composition of PIB, and the second one the complementary PDMS content.

Table 1 reports the main physical properties of PIB and PDMS at the reference temperature of 23 °C. A more complete characterization of the rheology of the

Table 1 Physical properties of the PIB/PDMS system at T=23°C

	Newtonian viscosity η_0 (Pa s)	density ρ (kg/m^3)	Refractive index n	Interfacial tension σ (N/m)
PIB	93	894	1.499	3.0×10^{-3}
PDMS	197	971	1.406	

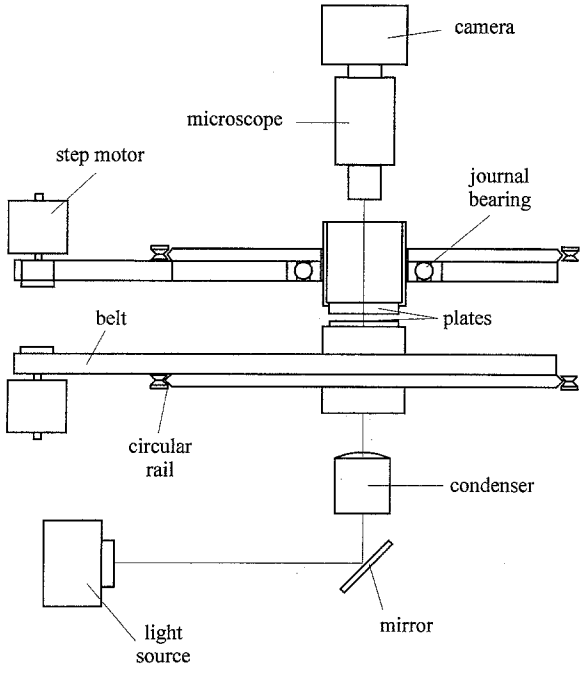

Fig. 1 Schematic view of the counter-rotating parallel plate apparatus

pure components and of their interfacial behavior can be found elsewhere (Sigillo et al. 1997). The zero shear rate viscosity of PDMS is about two times that of PIB, and in all the experiments reported in this paper the shear rate never exceeded the Newtonian limit for both polymers. Dynamic experiments showed also that PDMS is characterized by an elasticity higher than PIB, although its absolute value remains very low at frequencies corresponding to the low shear rate limit. It can be concluded that, at least in the shear rate range used in the experiments, the two polymers can be regarded as Newtonian.

In situ morphology measurements were performed on a home-made apparatus (schematically depicted in Fig. 1), constituted by two rotating optical windows of 50 mm diameter and 3 mm thickness (Melles Griot BK7). Each plate is glued on top of a hollow cylindrical holder, which screws into the central hole of a tilting journal bearing. The precision screw controls the vertical movement of the plates, and it is used to set the sample gap thickness; the tilting of the bearings is adjusted to guarantee parallelism (better than 10 μm) between the plates. The bearing itself seats in the central hole of a circular steel plate, which rotates on a peripheral, high precision circular rail. Each rotating unit is belt-driven by a computer-controlled step motor. A gearbox coupled to the motor, along with the belt reduction ratio, determines a rotation speed of the plates in the range 0.01–0.5 rad/s. The two rotation units can move along precision rectilinear rails, which are used to set the coaxiality of the two independent rotation axes to better than 5 μm.

Microscopic observations during flow were performed by means of a B/W CCD camera (Hitachi KP-ME1, 768×493 pixels), attached to a microscope tube (Melles Griot 04 TCF 002). Transmitted light through the sample was provided by an adapted microscope lamp (Zeiss Axioscope 100 W) equipped with a long working distance condenser (Zeiss LD Kondensor, 0.3 H). Three objectives (Zeiss Achroplan, 10× and 20× magnification, and Leitz, long working distance, 32× magnification) were used, depending on the size of the dispersed phase. The microscope and the lamp can be moved simultaneously around the plates, thus allowing observations at different radial locations. Images were recorded on tape (professional SVHS recorder Panasonic AG 7355) for later analysis, which was carried out by a PC-hosted frame grabber (Data Translation DT-2867-LC) equipped with a suitable software (Global Lab Image by Data Translation).

The counter-rotation of the two plates makes it possible to follow flow-induced events (such as deformation, breakup, coalescence) on the same drops for an ideally indefinite time (in practice, mechanical misalignments limit this "freezing effect" to a finite, though long, time). The idea of using two plates moving in opposing directions to directly observe sheared liquids is not new. Taylor (1934) generated a shear flow between two oppositely translating bands. Karam and Bellinger (1968), among others, used counter-rotating cylinders to observe the deformation and breakup of droplets in Couette shear flow. More recently, Levitt et al. (1996) studied the effects of elasticity on the deformation behavior of isolated polymer droplets by means of a counter-rotating plate device similar to the one used in this work. As will be specified in a following section, the possibility of fixing the deformed drops with respect to the microscope point of view has been exploited to investigate the possible occurrence of migration phenomena.

Experimental results

Experimental procedure

In a typical experiment, the blend was loaded in the apparatus and the gap between plates was set. A "clearing" flow condition was then applied, that is, a

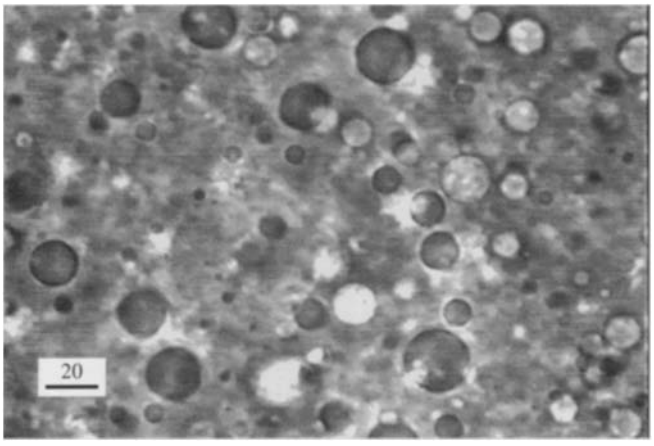

Fig. 2 Morphology of a 10/90 PIB/PDMS blend. Step-down from 3 to 0.3 s^{-1}. The image has been taken at 3000 strain units after step-down. The bar on the left represents a length of 20 μm

high rotation speed of the plates was imposed (typically, for a 1 mm gap, a shear rate at the edge of ca. 25 s^{-1} is obtained) for a time of at least 10 min. Under these conditions, the blend rapidly became very turbid and drops of the dispersed phase could not be recognized through the microscope, since most of them fell in the sub-micron size range. The rotation speed was then stepped down, and the morphology evolution was observed. Since for a parallel plate geometry the shear rate increases linearly along the plate radius, the morphology at different shear rates could be explored by simply moving the microscope at different radial positions along the sample. After step-down the sample turbidity decreased gradually, and larger droplets began to appear, thus confirming that the dominant phenomenon taking place in the blend was coalescence. For shear rates larger than 1 s^{-1} and concentrations greater than ca. 10%, however, the microscope images did not allow a quantitative analysis of the morphology. In fact, either a shear rate too high generated droplets too small to be measured, or high concentrations made the dispersed phase too "crowded". In both cases the blend was too turbid for an accurate size measurement.

A typical microscope image of the blend morphology is shown in Fig. 2 for a 10/90 blend. The blend has been "cleared" at 3 s^{-1}; after that, the shear rate has been stepped down to 0.3 s^{-1}. The image has been taken after 3000 strain units, that is, 10000 s after step-down. Droplets of PIB in the PDMS phase are clearly seen in Fig. 2. Their number and diameter can be easily obtained by the image processing software.

In order to verify that a steady-state morphology had been obtained, images of the sheared blend were taken at different times. The average size of the distribution was measured each time over a population of at least 150 droplets. Steady-state conditions were considered to be reached when no further change of the average drop size with time could be detected. Due to the extremely long transient times, experienced in particular at low concentrations and low shear rates (Vinckier et al., 1997), the attainment of a steady-shear morphology was verified over times of the order of some days.

The blend morphology has been characterized by its size distribution function $f(D)$, or by the corresponding cumulative distribution $F(D)$, where D is the drop diameter. Once $f(D)$ is known, average quantities can be computed. In particular, use will be made of the number-average and volume-average diameters, D_n and D_v, defined as:

$$D_n = \sum_i f(D_i)\, D_i = \frac{1}{N} \sum_i n_i D_i \tag{1}$$

$$D_v = \frac{\sum_i f(D_i)\, V_i D_i}{\sum_i f(D_i)\, V_i} = \frac{\sum_i n_i D_i^4}{\sum_i n_i D_i^3} \tag{2}$$

In Eqs. (1) and (2) D_i is the diameter of a generic drop, N is the total number of droplets, and n_i and V_i are the total number and total volume of the drops of diameter D_i, respectively.

Sources of error

Particular care has been taken in evaluating possible sources of error in the morphology measurements. End effects have been investigated by doing microscopy observations both near the sample edge and in the center of the rotating plates. Observations at the edge showed that some air bubbles were incorporated into the liquid, but remained confined in a thin layer of about 1 mm near the surface. Morphology measurements, therefore, excluded a radial region of about 5 mm from the edge. Similarly, measurements were not performed in a circle of about 5 mm around the plate center of rotation. In this region the shear rate is always relatively low, and the initial "clearing" procedure was not able to produce a sufficiently fine morphology. The distribution of drops determined during sample loading was found to persist even after shearing for long times at the maximum rotation speed, leading to unreproducible results in this region. The central area of the plates was also avoided in view of the possible spurious effects that the high curvature of the streamlines could generate on the deformation, breakup and coalescence phenomena. Since the clearance between the microscope objective and the plate holder limited the observations to a maximum radius of 20 mm, actual measurements were performed in a region defined by $5<r<20$, where r is the plate radius in mm units.

The possibility of counter-rotating the two plates was used to investigate possible migration effects in the

blend. The density difference $\Delta\rho$ between the dispersed and the continuous phase could generate sedimentation or buoyancy of the droplets, depending on the sign of $\Delta\rho$. At the same time, the curvature of the streamlines in the flow field could be responsible for the inward or outward migration of the drops. Migration along the radial direction was theoretically predicted by Chaffey et al. (1965). They found that, for Newtonian liquids of matching density, drops should move inwards or outwards depending on whether the ratio $p=\eta_d/\eta_m$ between the drop and the matrix viscosity is respectively larger or smaller than about 0.14. The same authors, however, were not able to confirm their prediction, since they found erratic, unreproducible experimental results.

The absence of migration effects of both types was verified by shearing a 5/95 blend at constant shear rate for long times. Drops of different sizes were focused under the microscope, and the rotation speed of the plates was set so as to keep the droplets within the objective field of view. Shear rates in the range 0.06–1.0 s^{-1} were applied. After several hours, no evidence of buoyancy could be found, as confirmed by the fact that the drops remained well focused by the microscope. Since drops could be seen to remain within the microscope field of view, systematic radial migration could also be excluded.

Another possible source of error in measuring the blend morphology is related to the fact that the droplets are deformed, under the action of shear, into elongated objects. Since the sample is observed along the gap thickness, that is, the velocity gradient direction, only a projection of the deformed drop is observable, and no accurate information on its actual size can be extracted from the image. This problem has been already pointed out by Takahashi and Noda (1995), who decided to use the small axis of the elongated drop as a measure of its size. In the present work, the droplet size was not measured directly during flow. On the contrary, images like that of Fig. 2 were obtained by stopping the flow only for a very short time (about 5 s), so that droplets could relax to the spherical shape, and their diameter could be measured. The flow was then resumed immediately after image acquisition. By repeating this procedure on different blends at different shear rates, it was carefully verified that this "stop-and-go" method did not interfere with the shear-induced morphology evolution. In fact, neither drop breakup nor coalescence were ever observed during the short time spent by the blend at rest.

Steady-state results. 10/90 blend

Most experiments performed in this work have been carried out on blends of 10% PIB volume fraction. Results for this blend are presented in this section. The effect of blend composition and phase inversion on the morphology will be presented in a subsequent section.

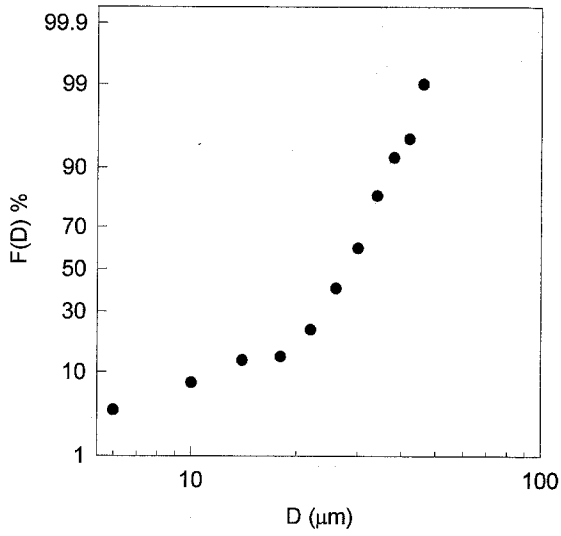

Fig. 3 Cumulative number distribution function vs. drop diameter for a 10/90 PIB/PDMS blend. Steady-state morphology at a shear rate of 0.26 s^{-1}

Figure 3 shows a typical example of the droplet cumulative distribution function in steady-state conditions; similar results have been found at all shear rates investigated. It is clear from Fig. 3 that the particle size does not follow a log-normal distribution. Rather, two distinct slopes can be observed, indicating the presence of a bimodal distribution, with dominance of larger droplets. A similar behavior has been already observed in situations where flow-induced coalescence takes place in the blend (Rivera-Gastélum and Wagner, 1996; Sundararaj and Macosko, 1995).

The size distribution function at steady-state is in any event relatively narrow. Indeed, it was found that the ratio between the volume-average and the number-average diameter, which can be taken as a global measure of the size polydispersity, was always only slightly larger than one. It can be concluded that either D_n or D_v can be indifferently used as a measure of the average size of the distribution.

All experimental data obtained for the 10/90 blend are summarized in Fig. 4. Here, the number-average diameter is plotted as a function of shear rate. Symbols refer to different experimental runs: in each of them, the size distribution was measured at selected radial positions, corresponding to different shear rates. By changing either the plate rotation speed or the gap thickness, the same shear rate could be obtained at a different radius. The data of Fig. 4 show the good reproducibility of the measurement. In particular, the results are not affected by a change of either rotation speed or sample thickness. This fact indirectly confirms the absence of radial drop migration in the sheared blend, and indicates also that the steady-state morphology is not affected by the macroscopic size of the sample.

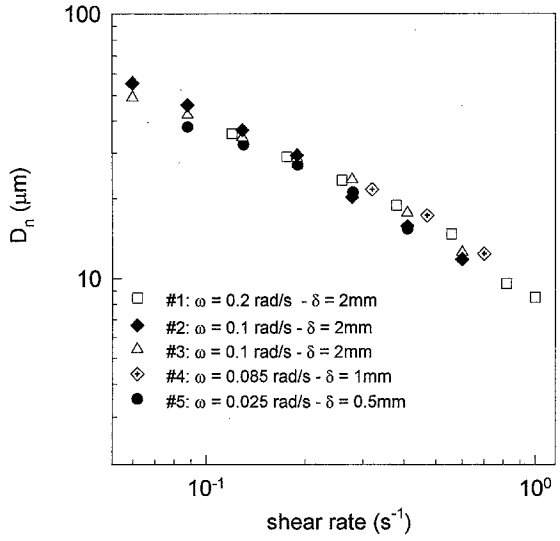

Fig. 4 Number-average drop diameter as a function of shear rate for the 10/90 blend. Symbols refer to different experimental runs as specified in the legend

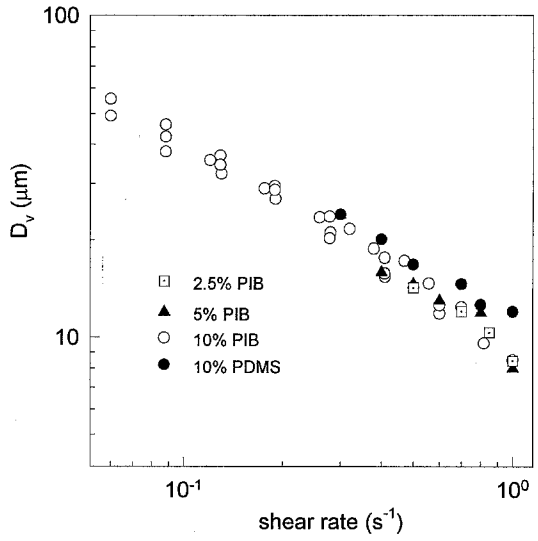

Fig. 5 Number-average drop diameter as a function of shear rate for PIB/PDMS blends of different compositions

Figure 4 shows that the average steady-state drop size is a decreasing function of shear rate. From the qualitative point of view this is an expected result, as confirmed by several studies on the morphology of sheared blends (see, for example, Elmendorp and Van der Vegt, 1986; Wu, 1987; and more recently Tsai and Min, 1995; and Rivera-Gastélum and Wagner, 1996). All the literature data, however, with the exception of those by Takahashi and Noda (1995), have been obtained by analyzing the blend morphology after flow on solidified samples.

The results of Fig. 4 can be directly compared with those obtained on the same blend by Vinckier et al. (1996). They estimated the average size of the same 10/90 PIB/PDMS blend from dynamic rheological experiments performed after cessation of a steady shear flow. Good quantitative agreement is found in the overlapping range of shear rates (compare Fig. 8 of Vinckier et al., 1996), at least when the viscoelastic data are translated into a volume-average drop size by using a direct fit of the Palierne model for Newtonian emulsions (Palierne, 1990; Graebling et al., 1993).

Effect of blend composition and phase inversion

The effect of blend composition on the average drop size is shown in Fig. 5. Data for the 5/95 and 2.5/97.5 blends are restricted to the high shear rate of the experimental window, due to the slow evolution kinetics of these more diluted systems (Vinckier et al., 1997).

Figure 5 shows that the average drop size does not depend on blend composition at steady-state. This is somewhat surprising, and apparently not in agreement with typical results presented in the literature. One might expect that, by increasing the composition of the dispersed phase, the probability of collision between droplets would increase as well. This argument has been used, among others, by Elmendorp and Van Der Vegt (1986) and by Sundararaj and Macosko (1995) to justify the observed increase in average drop size as a function of concentration in flowing polymer blends. It must be said, however, that Elmendorp and Van der Vegt (1986) used a single screw extruder, and Sundararaj and Macosko (1995) used either a batch mixer or a twin screw extruder. In all cases, these apparatuses are characterized by complex flow fields, where both variable shear and extensional components are present. Furthermore, it can be argued that in these experiments the blend morphology has not reached real steady-state conditions. In fact, transient experiments show that long times are necessary to get a stationary morphology at constant shear rate, and that the kinetics are a strong (quadratic) function of blend composition (Vinckier et al., 1997). This point will be further considered in the following section.

Figure 5 shows also that no qualitative changes in the size vs. shear rate behavior are observed when the two phases are inverted. Droplets of PDMS in the continuous PIB matrix seem to be only slightly larger than PIB drops at the same shear rate. This result is also in agreement with those obtained by Vinckier et al. (1996) from dynamic rheological tests.

As a final remark it must be said that, for all shear rates and compositions investigated, no fibrillar structures were observed during flow in steady-state condi-

tions. Even the largest droplets appeared only slightly elongated, and they all relaxed to the spherical shape after stopping the flow. This point is of importance in evaluating the physical mechanisms leading to the stationary morphology, as will be discussed below.

Discussion

The experimental results presented in the previous section can be summarized as follows: i) after a step-down in shear rate the average size of the blend increases, indicating that coalescence events control the transient evolution of the morphology; ii) when steady-state conditions are reached, the drop size is a decreasing function of shear rate; iii) the steady-state size does not depend upon blend composition, at least when PIB is the dispersed phase and its volume fraction is less than 10%; iv) no fibrillar domains are observed over the whole range of shear rates and compositions investigated. In order to interpret these results, both physical phenomena taking place in a sheared blend, that is, breakup and coalescence, must be considered.

The breakup of a single droplet of diameter D in shear flow is controlled by the balance between viscous and interfacial stresses. The resulting dimensionless parameter is the well known Capillary number, Ca:

$$\mathrm{Ca} = \frac{\eta_m \dot{\gamma} D}{2\sigma} \tag{3}$$

For small Ca, the two stresses balance each other, which results in a deformed drop; for large Ca, viscous stresses dominate, causing the irreversible deformation of the drop, which will eventually breakup into smaller domains. A critical Capillary number, Ca_c marks the separation between these two possible situations. Estimates for Ca_c have been first given by Taylor (1934). Decades later, Grace (1982) experimentally measured Ca_c over a wide range of shear rates and viscosity ratios. His results showed that Ca_c is a strong function of the viscosity ratio, p, and reaches a minimum for $p \approx 1$. This means that the most favorable conditions for breakup are found when the dispersed and the continuous phase have about the same viscosity. In the range $p<1$, the results of Grace substantially confirmed the theoretical predictions derived earlier by Acrivos and Lo (1978).

Since Ca_c depends only on the viscosity ratio, a critical diameter D_c can be defined at each shear rate such that, for $D<D_c$, drops will only deform, whereas for $D>D_c$ breakup will take place. According to Eq. (3), D_c can be expressed as:

$$D_c = \mathrm{Ca}_c(p)\frac{2\sigma}{\eta_m}\frac{1}{\dot{\gamma}} \tag{4}$$

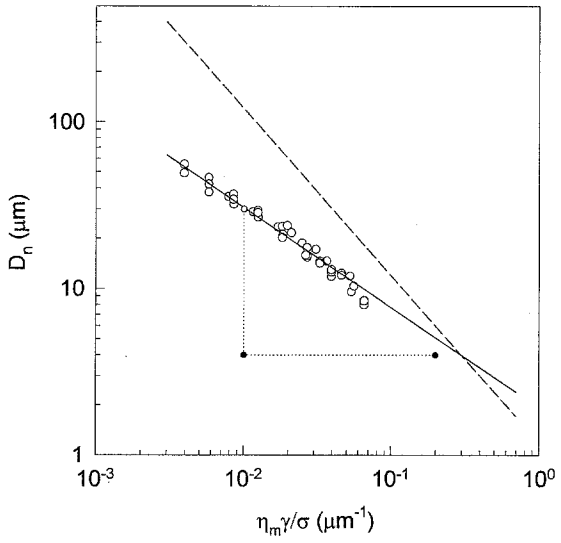

Fig. 6 Number-average drop diameter as a function of the group $\eta_m \dot{\gamma}/\sigma$ for blends having PIB as the dispersed phase. Symbols are experimental data. Broken line: D_c for breakup, Eq. (4) in the text. Solid line: Janssen model for coalescence, Eq. (5) in the text. The two dotted line represents an ideal "trajectory" of the morphology evolution during the step-down experiment

When plotted on a log-log plot of the drop diameter against the quantity $\eta_m \dot{\gamma}/\sigma$, Eq. (4) is a straight line of slope −1, whose absolute position is determined by the value of Ca_c, that is, by the blend viscosity ratio. For PIB/PDMS blends, where PIB is the dispersed phase, Eq. (4) is shown in Fig. 6. In this case, the viscosity ratio (see Table 1) is $p=0.47$. For this value of p the data of Grace (1982), as well as single drop experiments on the same system used in this work (Guido, 1996), indicate a value of Ca_c of about 0.6.

In Fig. 6 the same data of Fig. 5 are replotted in terms of the new variable $\eta_m \dot{\gamma}/\sigma$. It is clear that the average size of the droplets falls well below the critical curve for breakup, immediately suggesting that breakup phenomena are not effective in determining the steady-state morphology of the blend. One can assume that after the step-down in shear rate, coalescence events generate an increase in the average drop size, but this growth stops without producing droplets large enough to be again broken up by the action of flow. This picture can also justify the experimental observation (already reported above) that no fibrillar structures are observed under stationary conditions. Indeed, if the drop size remains sufficiently small at a given shear rate, the corresponding Ca_c will never be reached, and no drops would undergo an irreversible deformation.

The hypothesis that drop breakup does not take place in the sheared blend has been confirmed by performing the following experiment. A steady-state morphology has been obtained at a fixed shear rate, according to the step-down experimental procedure. Then,

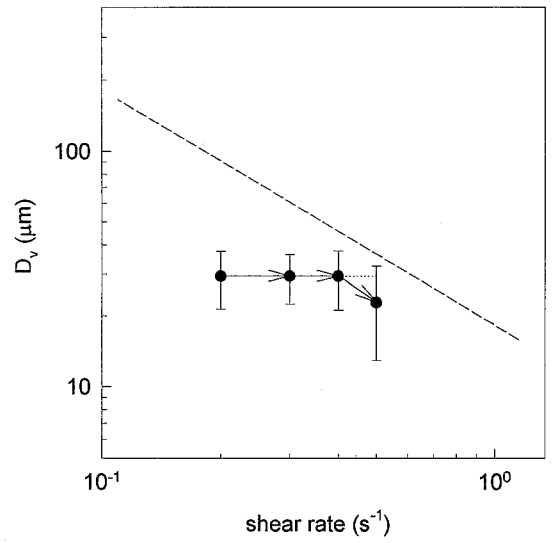

Fig. 7 Number-average diameter as a function of shear rate for a 10/90 blend in a sequence of succesive step-ups in shear rate. The solid line is the limiting condition for breakup, Eq. (4) in the text

gradual step-ups in shear rate have been imposed on the sample, and the average steady-state size has been correspondingly measured. The results of this experiment are shown in Fig. 7, for a 10/90 blend, in terms of number-average diameter vs. shear rate. Here, the starting point is the stationary morphology at 0.2 s^{-1}. Subsequent setp-ups to 0.3 and 0.4 s^{-1} do not show any change in the average drop size. Only when the shear rate is further stepped up to 0.5 s^{-1}, a clear decrease in the average size can be observed. It should be noticed that the error bars in Fig. 7 correspond to twice the standard deviation of the distribution, and that the decreasing straight line represents again the critical diameter for breakup, as predicted from Eq. (4). The optical observations show that, only when the shear rate approaches the value for which the measured diameter satisfies Eq. (4), elongated filaments begin to form, and breakup of the larger drops takes place. As a consequence, the average diameter decreases and the distribution broadens, as confirmed by the larger error bar at 0.5 s^{-1}.

The experiment reported in Fig. 7 constitutes the final evidence that, at least in the conditions investigated here, the steady-state morphology is not affected by breakup phenomena. As a consequence, only coalescence events are of importance under these conditions. Such a physical situation has been already predicted by Elmendorp and Van der Vegt (1986), who proposed a model for drop coalescence in Newtonian dispersions undergoing simple shear flow. For simplicity, all drops are assumed to have the same diameter. Coalescence is generated by collisions between droplet pairs moving at different relative velocities in the flow field. Not all collisions, however, are effective in producing coalescence, which takes place only when the draining of the continuous phase "trapped" between the drops is fast enough. The authors assumed coalescence only when the liquid gap between two droplets, h, would fall below a critical value, h_c, during the approaching stage. The predictions of the model showed that the probability of coalescence is a function of the Capillary number Ca, of the critical gap h_c, of the nature of the interface, but also of the absolute size of the droplets. In particular, all other parameters being fixed, the model predicted that coalescence does not take place when the drop diameter exceeds a limiting value, D_{coal}, and that such a diameter is a decreasing function of the applied shear rate.

The model of Elmendorp and Van der Vegt (1986) was derived only for the limiting cases of fully mobile and fully immobile interfaces. Furthermore, a closed-form relationship between D_{coal} and the shear rate was not derived. More recently, an improved model has been proposed by Janssen (1993), which incorporates the more realistic assumption of partially mobile interfaces, thus accounting also for a finite viscosity ratio. The model provides the following explicit expression for D_{coal}:

$$D_{coal} = 2p^{-\frac{2}{5}}\left(\frac{4}{\sqrt{3}}h_c\right)^{\frac{2}{5}}\left(\frac{\eta_m\dot{\gamma}}{\sigma}\right)^{-\frac{3}{5}} \tag{5}$$

Equation (5) implies a power-law dependence of D_{coal} on the characteristic group $\eta_m\dot{\gamma}/\sigma$, with an exponent of –0.6.

In Fig. 6 the predictions of Eq. (5) are directly compared to the experimental data for blends where PIB is the dispersed phase. The solid line is the best fit of the Janssen model, where the critical thickness h_c is taken as the only adjustable parameter. The number-average diameter correctly follows the power-law dependence expressed by Eq. (5). Quantitative agreement is obtained with a value of critical thickness given by h_c=0.2 μm. Although very few data are available in the literature for h_c, the value can be considered as reasonable. Indeed, a value of h_c=0.05 μm is reported for drops coalescing on a flat surface in water/oil systems (MacKay and Mason, 1963).

An independent check of the model of Janssen is shown in Fig. 8, where PDMS is now the dispersed phase. Since the viscosity ratio is in the case p=2.1, both limiting curves for breakup and coalescence, given by Eqs. (4) and (5), must be modified accordingly. By keeping the value of h_c from the previous best fit, it is found in this case that the model of Janssen slightly underestimates the average droplet size, but the data still follow the expected power-law dependence from the group $\eta_m\dot{\gamma}/\sigma$. It must be noticed that a regression of the data in Fig. 8 with Eq. (5) would yield a value of h_c=0.26 μm.

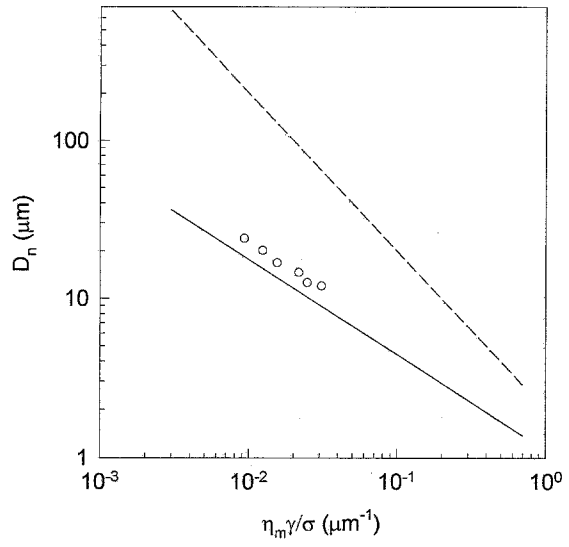

Fig. 8 Number-average drop diameter as a function of the group $\eta_m \dot{\gamma}/\sigma$ for a 90/10 blend, having PDMS as the dispersed phase. Symbols and lines as in Fig. 6

To graphically summarize the physical behavior of the PIB/PDMS blend in the experimental conditions applied in this work, one can again refer to Fig. 6. This figure (as the equivalent Fig. 8 for PDMS drops) represents a sort of "phase diagram" to predict the shear-induced morphology of PIB droplets in PDMS. Similar diagrams can be found in Elmendorp and Van der Vegt (1986) in Janssen (1993) and in Utracki and Shi (1992). In the present work, however, direct comparison is provided for the first time with experimental data.

When performing a step-down in shear rate, the initial condition is represented by the black dot in the lower-right part of the figure: due to the high shear rate applied to the system a small size morphology is developed in the blend. When the shear rate is suddenly reduced, the system is represented by the black dot in the lower-left side. The shear rate is now too low to induce anything but coalescence events: the system evolves by moving upwards along the vertical line, until it reaches the limiting diameter for coalescence. At this point, further coalescence is inhibited by the large drop size, but the latter is still too small to generate breakup. The system, therefore, sits in a "dead" steady-state condition, which has been determined only by coalescence.

It can now also be understood why the stationary morphology does not depend on blend composition. This parameter, in fact, is expected to affect only the kinetics of the transient morphology evolution. Less concentrated blends will reach steady-state conditions in a longer time, but the final morphology will be always the same, once the quantity $\eta_m \dot{\gamma}/\sigma$ has been fixed.

To conclude this section, it must be pointed out that, as the magnitude of the group $\eta_m \dot{\gamma}/\sigma$ is increased, Fig. 6 shows that the two limiting curves for coalescence and breakup will cross at some point. This means that, for sufficiently high values of shear rate, the mechanism leading to steady-state will change from a "coalescence-controlled" to a "breakup-controlled" one. In fact, if a sufficiently high shear rate is imposed (in particular, for the diagram in Fig. 6, if $\eta_m \dot{\gamma}/\sigma$ is greater than about 0.3), the limiting curve for breakup will be encountered first, and the size of the steady-state morphology will be limited by breakup events. Only in this case, therefore, a real "dynamic equilibrium" between coalescence and breakup is expected. Unfortunately, optical microscopy observations are unable to explore this range of the blend phase diagram, since the absolute size of dispersed phase is too small to be resolved by the microscopy images. Very recently, however, this hypothesis has been confirmed by indirect average size measurements from dynamic rheological experiments performed on a similar blend (Minale et al., 1996).

Conclusions

The main result of this work is a clear and direct confirmation of the important role played by coalescence in determining the morphology of a flowing blend. In particular, experimental validation has been given for the first time to the theory developed by Elmendorp and Van der Vegt (1989), and later refined by Janssen (1993). Such a theory predicts that coalescence is inhibited, at low shear rates, when the drop size exceeds a critical value. As a consequence of the arrested drop size growth, breakup phenomena play no role in determining the steady-state morphology, which is controlled by coalescence only.

The experiments performed in this work have indeed confirmed the model predictions, and good quantitative agreement has been found between theory and experimental results. In the range of shear rates investigated, it was proved that the steady-state morphology of PIB/PDMS blends is fully controlled only by coalescence. The experimental window where such a behavior is observed was found to depend on both the physical properties of the system and the initial conditions imposed on the blend. On the contrary, as it can be also deduced by the model, the steady-state morphology was found not to depend on blend composition, at least in the concentration range investigated.

Acknowledgments This work has been partially supported by the European Union, under the BRITE-EURAM Program (Contract BRE 2.CT 02 9213), and by the Italian Ministero dell'Università e della Ricerca Scientifica e Tecnologica (MURST), 60% funds. The authors wish to thank Prof. P. Moldenaers and Prof. J. Mewis for the stimulating discussions.

References

Acrivos A, Lo TS (1978) Deformation and breakup of a single slender drop in an extensional flow. J Fluid Mech 86:641–672

Chaffey CE, Brenner H, Mason SG (1965) Particle motions in sheared suspensions. XVII: Deformation and migration of liquid drops. Rheol Acta 4:56–63

Chin HB, Han CD (1980) Studies on droplet deformation and breakup. II. Breakup of a droplet in nonuniform shear flow. J Rheol 24:1–37

Cogswell FN, Griffin BP, Rose JB (1983) US Patent 4386174

Collyer AA (1996) The morphology and rheology of liquid crystal polymer blends. In: Acierno A, Collyer AA (eds) Rheology and processing of liquid crystal polymers. Chapman and Hall, London, pp 185–217

Elmendorp JJ, Van der Vegt AK (1986) A study on polymer blend microrheology: part IV. The influence of coalescence on blend morphology origination. Polym Eng Sci 26:1332–1338

Elmendorp JJ (1991) Dispersive mixing in liquid systems. In: Rauwendaal C (ed) Mixing in polymer processing. Marcel Dekker, New York, pp 17–100

Favis BD, Chalifoux JP (1987) The effect of viscosity ratio on the morphology of propylene/polycarbonate blends during processing. Polym Eng Sci 27:1591–1600

Gauthier F, Goldsmith HL, Mason SG (1971) Particle motions in non-Newtonian media. I: Couette flow. Rheol Acta 10:344–364

Grace HP (1982) Dispersion phenomena in high viscosity immiscible fluid systems and applications of static mixers as dispersion devices. Chem Eng Commun 14:225–277

Graebling D, Muller R, Palierne JF (1993) Linear viscoelastic behavior of some incompatible polymer blends in the melt. Interpretation of data with a model of emulsion of viscoelastic liquids. Macromolecules 26:320–329

Guido S, private communication

Janssen JMH (1993) Dynamics of liquid-liquid mixing. PhD Thesis, University of Technology, Eindhoven, The Netherlands

Karam HJ, Bellinger JC (1968) Deformation and breakup of liquid droplets in a simple shear field. I&C Fund 7:576–581

Krause S (1978) Polymer-polymer compatibility. In: Paul DR, Newman S (eds) Polymer blends. Academic Press, New York, pp 16–113

Levitt L, Macosko CW, Pearson SD (1996) Influence of normal stress difference on polymer drop deformation. Polym Eng Sci 36:1647–1655

Lingaae-Jorgensen J, Utracki LA (1991) Makromol Chem Macromol Symp 48/49:189

MacKay GDM, Mason SG (1963) The gravity approach and coalescence of fluid drops at liquid interfaces. Canadian J Chem Eng 1:203–212

Minale M, Moldenaers P, Mewis J (1996) Morphological memory effects in polymeric blends, presented at the Dutch Society of Rheology Meeting, Oct 23, 1996

Palierne JF (1990) Linear rheology of viscoelastic emulsions with interfacial tension. Rheol Acta 29:204–214

Rivera-Gastélum MJ, Wagner NJ (1996) A rheological and morphological study of a copolyester liquid crystal/polypropylene blend system. J Polym Sci: Polym Phys 34:2433–2445

Sigillo J, di Santo L, Guido S, Grizzuti N (1996) Comparative measurements of interfacial tension in a model polymer blend. Polym Eng Sci, in press

Sundararaj U, Macosko CW (1995) Drop breakup and coalescence in polymer blends: the effects of concentration and compatibilization. Macromolecules 28: 2647–2657

Takahashi Y, Noda I (1995) In: Nakatami AI, Dadmun MD (eds) Domain structures and viscoelastic properties of immiscible polymer blends under shear flow. Flow induced structure in polymers. ACS Washington, pp 140–152

Taylor GI (1934) The formation of emulsions in definable fields of flow. Proc R Soc London A 146:501–523

Tsai HY, Min K (1995) The flow-induced phase morphology of fluoroelastomer and polycarbonate blends during extrusion. Polym Eng Sci 35:619–636

Utracki LA (1989) Polymer alloys and blends. Hanser Publishers, Munich

Utracki LA, Shi ZH (1992) Development of polymer blend morphology during compounding in a twin-screw extruder, Part I, II and III. Polym Eng Sci 32:1824–1856

Vinckier I, Moldenaers P, Mewis J (1996) Relationship between rheology and morphology of model blends in steady shear flow. J Rheol 40:613–631

Vinckier I, Terracciano AM, Moldenaers P, Grizzuti N (1997) Flow induced coalescence in immiscible polymer blends. AIChE J (submitted)

Wu S (1987) Formation of dispersed phase in incompatible polymer blends: interfacial and rheological effects. Polym Eng Sci 27:335–343